Nanocomposite membranes from nano-particles prepared by polymerization induced self-assembly and their biocidal activity

Lakshmeesha Upadhyaya, Beatriz Oliveira, Vanessa. Pereira, Maria Barreto Crespo, João Crespo, Damien Quemener, M. Semsarilar

Nanocomposite membranes from nano-particles prepared by polymerization induced self-assembly and their biocidal activity

Lakshmeesha Upadhyaya[a, †], *Beatriz Oliveira*[b,c], *Vanessa.J.Pereira*[b,c], *Maria T. Barreto Crespo*[b,c], *João G. Crespo*[d], *Damien Quemener*[a], *Mona Semsarilar*[a*]

[a]Institut Européen des Membranes, IEM, UMR 5635, Université de Montpellier, ENSCM, CNRS, Place Eugène Bataillon, 34095 Montpellier Cedex 05, France

[b]iBET - Instituto de Biologia Experimental e Technologica, Av Republica, Qta do Marques, 2780-157, Oeiras, Portugal

[c]Instituto de Tecnologia Química e Biológica António Xavier, Universidade Nova de Lisboa, Av. da República, 2780-157 Oeiras, Portugal

[d]LAQV- REQUI*M*TE, Departamento de Química, Faculdade de Ciências e Tecnologia, Universidade Nova de Lisboa, Campus de Caparica, 2829-516 Caparica, Portugal

Corresponding Author: (M.S.) E-mail: mona.semsarilar@umontpellier.fr.

Current address:

†King Abdullah University of Science and Technology (KAUST), Biological and Environmental Science and Engineering Division, Advanced Membranes and Porous Materials Center, 23955-6900, Thuwal, Saudi Arabia.

ABSTRACT

Silver ions have been widely used because of their antimicrobial properties. This study describes the production of novel nanocomposite membranes from a block copolymer and silver nanoparticles (NPs). These composite membranes display properties from both polymeric and inorganic materials along with the biocidal features obtained due to the presence of silver ions. The spin coating technique is employed to synthesize the nanocomposite membrane consisting of positively charged inorganic NPs and negatively charged polymeric NPs. Polymeric NPs of spherical, wormicular, and vesicular morphologies were synthesized using Reversible addition-fragmentation chain transfer (RAFT) polymerization using poly(methacrylic acid)-*b*-(methyl methacrylate) diblock copolymer. The silver NPs coated with poly(methacrylic acid)-*b*-poly(quaternized 2-(dimethylamino)ethyl methacrylate), were synthesized using a nanoprecipitation method. The silver NPs act as the bridging entity between the polymeric NPs, as well as conferring the antimicrobial activity to the composite membranes. To test their antimicrobial properties, membranes were incubated with *Enterococcus hirae.* Comparison with the controls shows a 2 to 3 log decrease in the bacterial count for a contact time of 24 h. Furthermore, membrane filtration experiments conducted with phosphate buffer saline solutions spiked with bacteria indicated the importance of incorporating silver NPs in the nanocomposite membrane to achieve considerable rejection of bacteria as well as biocidal activity.

KEYWORDS. Nanocomposite membranes, block copolymers, silver nanoparticles, biocidal activity

1. INTRODUCTION

Block copolymers are one of the remarkable contenders for the fabrication of polymeric membranes due to their ability to form well organized porous structures with exceptional mechanical stability [1–11]. There are many approaches available for the preparation of block copolymer-based membranes, like spin coating, extrusion, and bulk evaporation [1,12]. Several different research groups have developed various routes for the fabrication of asymmetric isoporous membranes from block copolymers via traditional non-solvent induced phase separation technique [4–6,8–10,13–15].

As previously reported[2,4–7,16], we have developed a new strategy to make membranes from block copolymer NPs of different morphologies (spherical, wormicular, and vesicular). The morphologies mentioned above were synthesized via an alcoholic RAFT dispersion polymerization [17]. The membranes from spherical NPs were more effective due to the arrangement of particles in a well-organized fashion, providing a uniform pore size across the membrane compared to membranes from other morphologies. To enhance the mechanical stability [18,19] of the membranes and confer them magnetic properties, iron oxide NPs bearing opposite surface charges were used to link the negatively charged polymeric NPs together. This strategy resulted in the successful preparation of nanocomposite magnetic membranes with a pore size that could be tuned via the application of magnetic fields of different strength [7]. Also, the use of the magnetic field successfully reduced protein fouling [7].

Membrane-based filtration techniques are up-and-coming in the area of water filtration for removal of microorganisms, organic pollutants, and inorganic compounds. Membrane processes like ultrafiltration and microfiltration have been successfully employed for water treatment [20,21]. In

water-based separation processes, biofouling may be one of the significant drawbacks due to the deposition of microorganisms like bacteria. After deposition, they may multiply at the membrane surface and produce extracellular material forming a biofilm and thereby affecting the membrane performance. The deposited materials will block the pores and thus decrease flux in a dramatic fashion [22,23].

Silver ions have been widely utilized as water disinfectant since their antimicrobial activity against a broad range of microorganisms has been well studied [18,19,24–26]. The antimicrobial property [27][27]of silver is mainly due to their interaction with protein thiol groups, which prevents DNA replication and affects the structure as well as the permeability of the bacteria cell membranes [28–32]. The incorporation of silver in membranes used for water treatment, to control biofouling, was previously studied.[24,25,32] Silver has been incorporated in membranes made from cellulose acetate, polyamide, poly(2-ethyl-2-oxazoline), polylactic acid [19,24–26,33–36], and Polyvinylidene fluoride (PVDF) [27]. Nunes et al. [32] used the polystyrene-*b*-poly(4-vinylpyridine) block copolymer for the fabrication of microporous membranes where the silver ions were deposited on the membrane surface and pore walls via chelation with the pyridine groups, facilitating the even distribution of the silver ions in the membrane. The NPs were deposited on the surface of the membrane at different pH values, and the ionic concentration of silver and its biocide activity was investigated using *Pseudomonas aeruginosa*. Chung et al.[27] blended the silver containing surface modifying macromolecule (SMMs) in PVDF forming PVDF membrane with surface migrated SMMs. Biofouling filtrations were conducted using *E.coli* spiked in synthetic wastewater as feed at a pressure of 50 psig. After 25 h of operation, the membranes were flushed with distilled water to recover the membranes. Due to the smaller pore size, the

solutes have been deposited on membranes contributing to flux reduction as well the membrane has shown greater antimicrobial properties due to the presence of silver ions on the surface.

In this work, we illustrate the fabrication of nanocomposite membranes from block copolymers in their spherical, wormicular, and vesicular morphologies and colloidally stable silver NPs. These membranes were prepared via spin-coating a blend of polymeric NPs and inorganic NPs (Silver particle coated with quaternized poly(2-(dimethylamino) ethyl methacrylate) in solution directly on a porous nylon support. The biocidal activity of selected membranes (from spherical polymeric NPs) was studied at different time intervals using a gram-positive bacterium, *Enterococcus hirae*.

2. EXPERIMENTAL

A detailed description of block copolymer synthesis along with materials and equipment used for experimentation are provided in supporting information (SI). The synthesis of silver NPs is explained below.

Silver NPs were synthesized using sodium borohydride ($NaBH_4$) as a reducing agent and 10 w/w% $PMAA_{47}$-*b*-$PQDMAEMA_{50}$ diblock copolymer as a stabilizing agent. The reduction procedure of silver nitrate ($AgNO_3$) was carried out at room temperature with the block copolymer as the stabilizing agent. A typical process is as follows: 1 mL of 10 w/w % aqueous solution of $PMAA_{47}$-*b*-$PQDMAEMA_{50}$ was added to 10 mL of distilled water under stirring. To this preparation, sodium borohydride in the molar ratio of 2:1 corresponding to silver nitrate was added. After the addition of the reducing agent, an aqueous solution of silver nitrate in the molar ratio of 3:1 corresponding to the diblock copolymer was added dropwise. During the addition of the silver nitrate solution, initially, the color of the reaction mixture changed to yellow and then browned. The reaction mixture was stirred for 30 min at room temperature followed by dialysis against water to remove unreacted reactants.

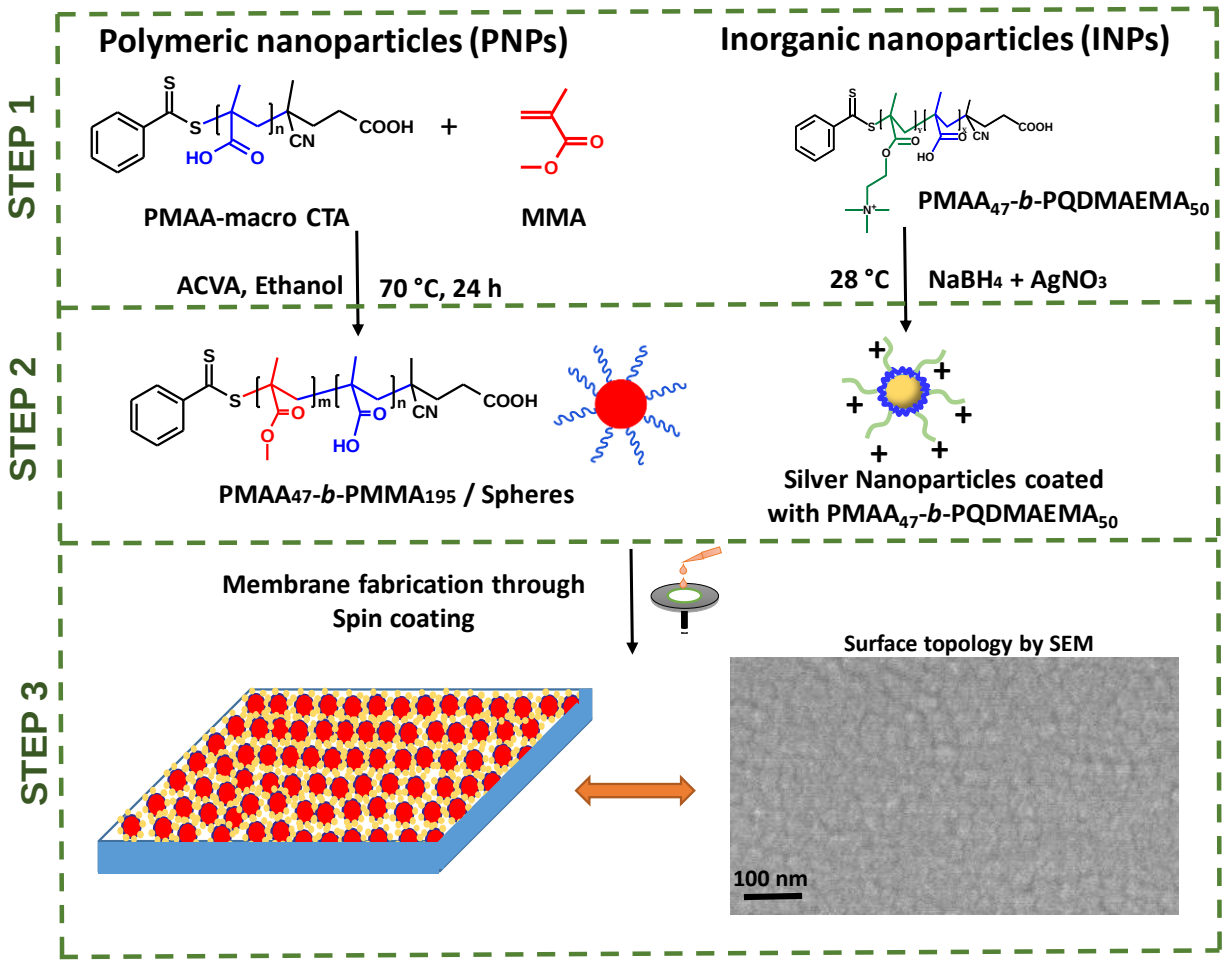

Scheme 1. Synthesis of polymeric NPs and silver NPs followed by nanocomposite membrane preparation via a spin coating technique.

2.1. Antimicrobial properties of membranes

2.1.1. Contact tests with bacterial solutions

The membranes were sterilized with absolute ethanol for 25 s followed by cleaning with sterile water before the contact experiments. Contact experiments (Scheme 2) were performed using 6 well cell culture plates where the three different membranes (nylon support, membrane without silver and membrane with silver) were immersed into 7 mL of sterile phosphate-buffered saline (PBS) solution spiked with a final concentration of $1x10^6$ CFU/mL of *Enterococcus hirae* (PBS). Controls containing only the bacteria spiked into sterile PBS were also performed to verify the

viability of the bacteria along the experimental time. Samples from the contact tests conducted with bacteria were analyzed immediately (0 h of contact) and after 1, 2, 4, 8, and 24 h of contact between the membranes and the bacteria. 3 mL of solution was collected from each well for the quantification of *Enterococcus hirae*. Serial dilutions were prepared with buffered water and incorporated (1 mL) into tryptone soy agar media in duplicate plates using the pour plate technique (Standard Method 9215B). Plates were incubated for two days at 37 °C, all the colonies counted, and the results obtained represented as CFU/mL.

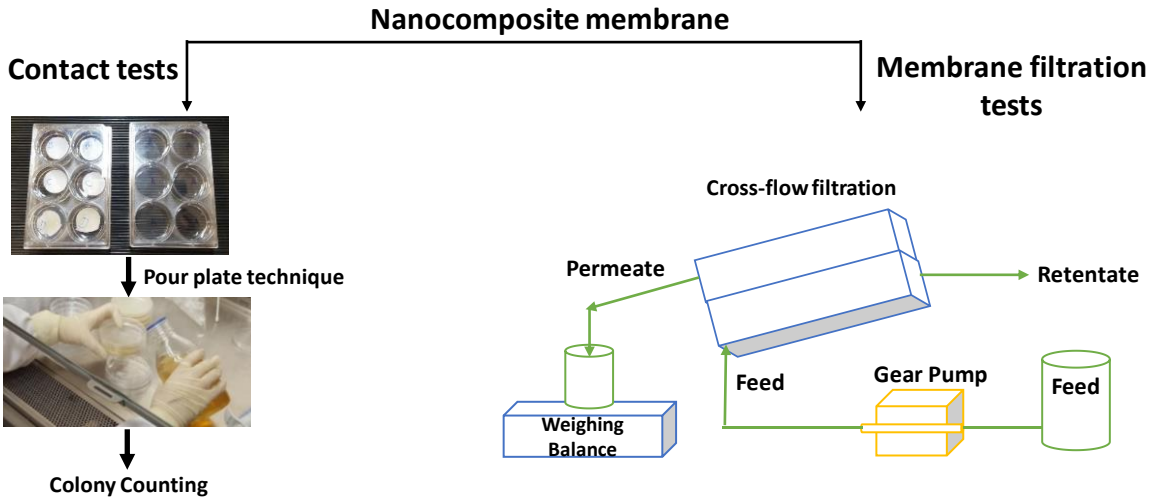

Scheme 2. Analysis of antimicrobial properties and membrane filtration of solutions spiked with bacteria using a cross-flow cell and a nanocomposite membrane made from spherical NPs of $PMAA_{47}$–*b*-$PMMA_{185}$ and silver NPs coated with $PMAA_{47}$-*b*-$PQDMAEMA_{50}$ chains.

2.1.2. Membrane filtration of bacterial solutions

For bacterial filtrations (Scheme 2), the cross-flow mode was selected and was conducted in a homemade cross-flow cell (Area of the membrane = 2.3 cm x 1.2 cm). The filtration experiments

were carried out at 1.5 bar of transmembrane pressure. Initially, the cross-flow cell, pump, tubings, and membranes were sterilized with absolute ethanol. 50 mL of phosphate-buffered saline (PBS) solution spiked with $1x10^6$ CFU/mL *Enterococcus hirae* was used as a feed solution. Feed, permeate, and retentate samples were analyzed for the different membrane filtration experiments (using the nylon support and the membrane immobilized with silver). 3 mL of each sample was used to prepare serial dilutions for quantification of *E. hirae*, in duplicate samples, using the pour plate technique and tryptone soy agar media.

3. RESULTS AND DISCUSSION

Previously, we demonstrated that nanocomposite membranes could be prepared from block copolymer NPs of different morphologies such as spheres, worms, and vesicles synthesized via RAFT dispersion polymerization (Scheme 1) and iron oxide NPs coated with positively charged poly(quaternized DMAEMA) [5,6]. It was demonstrated that the membranes made from a mixture of the diblock copolymer and iron oxide NPs had higher flux and constant permeability compared to membranes made from solely diblock copolymer particles. These nanocomposite membranes had excellent mechanical stability, as well as magnetic properties, overbear block copolymer membranes due to the presence of the magnetic iron-oxide NPs. In this work, we employ a similar strategy to prepare nanocomposite membranes containing silver NPs. The presence of silver NPs might confer antimicrobial properties to the membranes and help to suppress biofouling, which is the major problem associated with membrane processing in the form of fouling (partial or complete blockage of pores leading to flux reduction).

3.1.Silver NPs synthesis and characterization

Well defined silver NPs coated with the diblock copolymer ($PMAA_{47}$-*b*-$PQDMAEMA_{50}$) were synthesized by reduction of silver nitrate at room temperature. This is one of the first kind where the PISA formed polymer shells were decorated with block copolymer coated silver NPs. As shown in Fig. 1A, the hydrodynamic diameter of the silver NPs was 28.5 nm, as measured by DLS. The particle size distribution of 0.087 suggested the presence of near monodisperse particles. The calculated particle diameter at dry state (from TEM images) was 6.9 nm (Fig. 1B). TGA analysis (Fig. 1C) indicated a weight ratio of 16% silver to 84% of the diblock copolymer. The transmission electron microscopy images of these particles showed only spherical particles (no other morphologies such as hexagonal or cubic were observed). The positive zeta potential (+32.29 mV) confirmed the attachment of the diblock copolymer chains on the surface of the silver NPs via the negatively charged PMAA block.

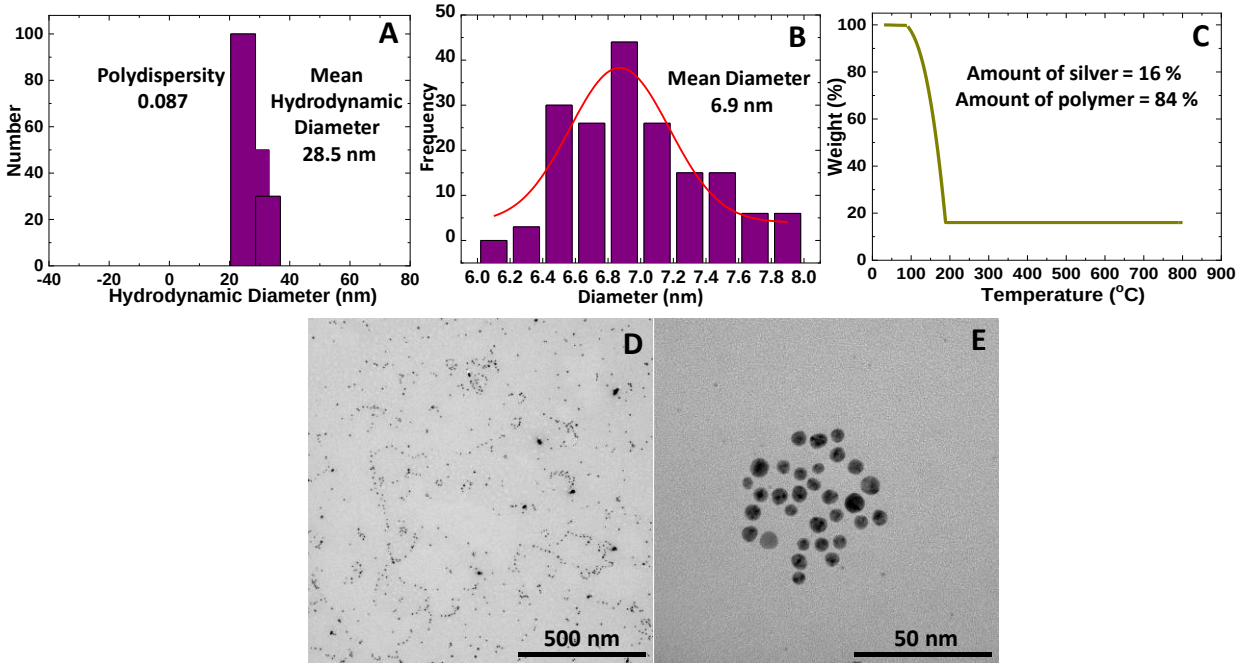

Fig. 1. Characterization of silver NPs: (A) Particle size distribution by DLS (B) Particle size distribution by TEM, (C) Thermogravimetric analysis and (D & E) TEM images.

3.2. Nanocomposite membrane synthesis and performance

The pure phases of spheres ($PMAA_{47}$-*b*-$PMMA_{195}$; Đ = 1.03, M_n = 21.3 kg/ mol), worms ($PMAA_{47}$-*b*-$PMMA_{273}$; Đ = 1.11, M_n = 28.6 kg/ mol) and vesicles ($PMAA_{47}$-*b*-$PMMA_{368}$; Đ = 1.21, M_n = 33.3 kg/ mol) with 17.5 wt.% of total solids content were used for the preparation of membranes (full characterization of the polymeric NPs could be found in Table S1). The selection of total solids content was random from the phase diagram from our previous work. The prepared membranes from 3 different particle morphologies were used in a cross-flow water filtration setup. During the filtration experiments, the following observations were made:

- For membranes from spheres, there was a decrease in the flux values as the pressure increased above 2 bar (Fig. S2A).
- For membranes from worms, a decrease in flux was not observed as pressure increased, but permeability has shown a decline phase (Fig. S3A), suggesting the movement of the top wormicular active layer into the sublayer, blocking the available pores.
- For membranes from vesicular NPs, the flux has shown a declining trend after applying 3 bar of pressure difference across the membrane (Fig. S4A).

This decrease is due to mechanical instability of the deposited polymer layer since, at high pressures, the polymeric particles get pushed into the nylon support layer, blocking the pores. This could be easily seen in the SEM images (Fig. S1), taken after filtration. The membranes from worms show larger pores at the top surface compared to others (Fig. 2C) but exhibit a lower flux. This may be due to their entangled substructure making the pores smaller compared to others.

To increase the cohesion between the particles and the mechanical stability of the deposited layer, positively charged silver NPs coated with $PMAA_{47}$-*b*-$PQDMAEMA_{50}$ were added to the formulation. To prepare the casting solution with a maximum amount of silver NPs, the isoelectric

point (where all the negative charges available on the polymeric NPs have been neutralized with positive charges of the silver NPs) of each dope solution was identified. For the polymeric colloidal solution of spheres, vesicles, and wormicular NPs (with a concentration of 6.7 mg/mL), 4.1, 3.1 and 2.1 mL of silver NPs (at 5.1 mg/mL) were required respectively to reach the isoelectric point. To avoid precipitation in the casting solution, the added volume of silver NPs was kept below the volume corresponding to the isoelectric point. For membranes containing spheres, initially, 1.3 mL of silver NPs was added to 1 mL of polymeric NPs. After water filtration tests, the SEM images suggested partial intrusion of the top active layer into the nylon support. This volume was then increased to 1.7 mL resulting in a stable top layer after filtration cycles up to 4 bar of transmembrane pressure (Fig. 2A & B).

Membranes from worms showed higher mechanical stability compared to those of spheres or vesicles due to their entangled structure. At 4 bar of transmembrane pressure, a slight change in permeability was observed. The addition of an extra 0.5 mL of silver NPs to the casting solution was enough to obtain a stable top layer that could stand 4 bar of pressure. In the case of membranes from vesicles, 1.3 mL of silver NPs were needed to prepare a stable layer. The SEM images of the tested membranes, after two cycles with a maximum transmembrane pressure of 4 bar, are shown in Fig. 2. The permeability and flux data obtained for these nanocomposite block copolymer membranes are shown in Fig. S2, S3 & S4 indicate that the strategy of adding silver NPs with opposite charge enhances the mechanical stability (tested up to 4 bar of transmembrane pressure) of the prepared membranes and is entirely dependent on the concentration of added silver NPs.

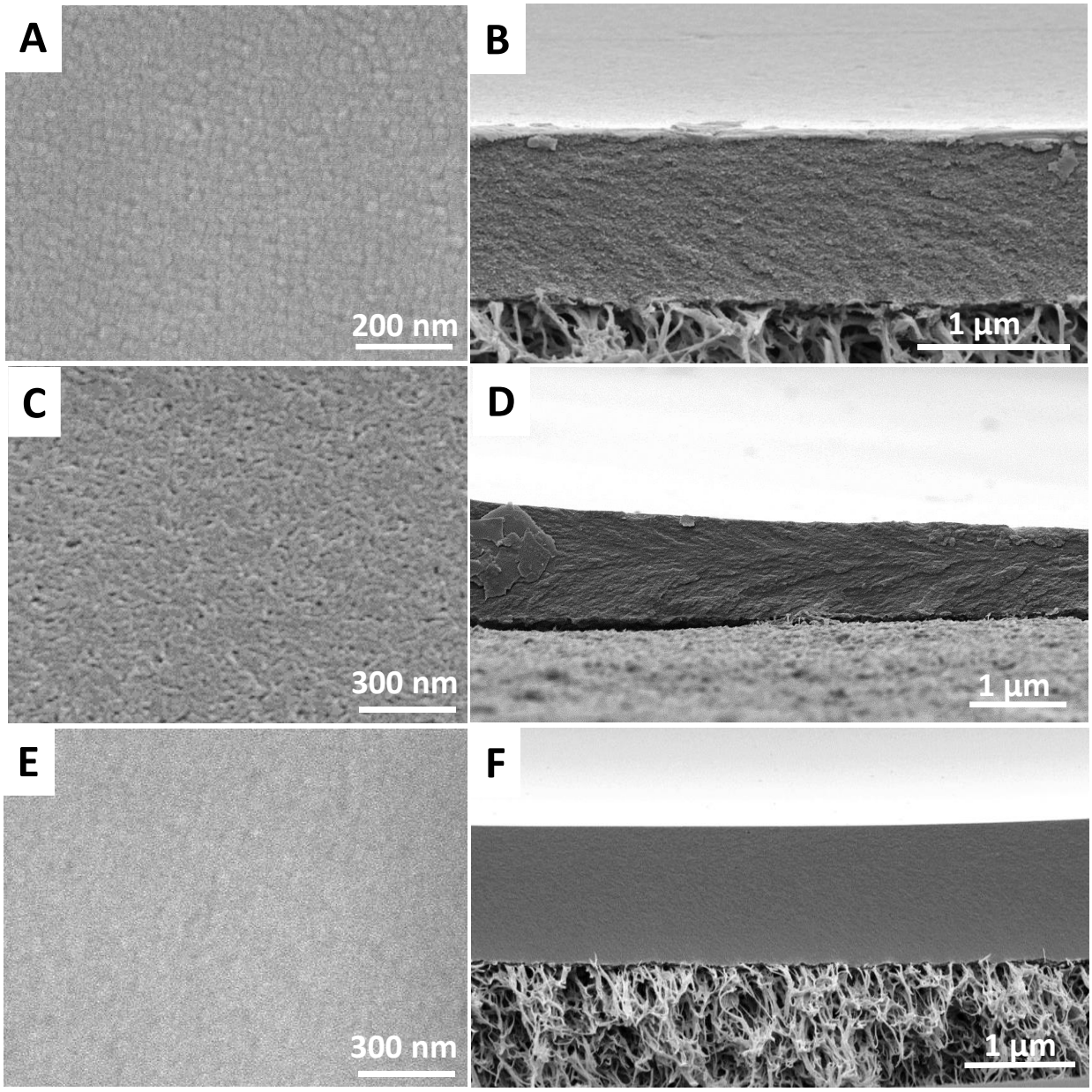

Fig. 2. SEM Images of thin-film block copolymer membranes top surface and cross-section prepared through spin coating on nylon film using (A & B) Spheres, $PMAA_{47}$-*b*-$PMMA_{195}$, (C & D) Worms, $PMAA_{47}$-*b*-$PMMA_{273}$ and (E & F) Vesicles, $PMAA_{47}$-*b*-$PMMA_{368}$.

After incorporation of the optimal amount of Silver NPs in the membranes, the flux values increased linearly with constant permeability, with TMP varying between 1- 4 bar. In the case of membranes from spherical particles, the flux value increased from 148.6 $L.m^{-2}.h^{-1}$ at 1 bar to 589.6

$L.m^{-2}.h^{-1}$ at 4 bar of TMP. When comparing this value with a similar magneto-responsive membrane [7] it could be seen that these fluxes are about 54-57% higher for both 1 bar and 4 bar TMP. The same trend (10-37% and 21-25% higher) was observed with membranes made from wormicular and vesicular NPs (Table 1).

Table 1. Comparison of water flux at pH 7.1 for membranes containing iron oxide and silver NPs

Pressure (Bar)	Flux ($L.m^{-2}.h^{-1}$)					
	Membranes from Spheres		Membranes from Worms		Membranes from Vesicles	
	Iron oxide NPs[6]	Silver NPs	Iron oxide NPs[6]	Silver NPs	Iron oxide NPs[6]	Silver NPs
1	96.5	148.6	55.6	61.3	85.3	103.3
4	375.3	589.6	152.7	209.3	328.3	411.9

The reason behind the increase in water flux is probably due to changes in hydrophilicity or due to the change in thickness of the membrane. Both the thickness and contact angle comparison have been depicted in table 2 for the membrane containing silver NPs and iron oxide NPs. The thickness is lower for membranes with silver compared to Iron oxide NPs. This change was not significant for membranes from spheres. So both thickness and contact angle may play a pivotal role for the higher fluxes observed in membranes containing silver, compared to those containing iron oxide NPs.

Water contact angles of the membranes could be used for the estimation of changes in surface hydrophilicity [37]. The contact angle of the membranes without any silver NPs was found to be 48°, which was decreased to 45° when Iron oxide NPs were incorporated in the membranes. This

number further changed to 39° when silver NPs were integrated. The possible explanation for changes in hydrophilicity may be due to the following reasons. In aqueous solution, due to oxidation, silver ions will be released by silver NPs. These released ions will be adsorbed on the surface of silver NPs forming a layer of hydrated silver ions, thereby changing the hydrophilicity of the layer. The dissolved oxygen concentration in water will also facilitate the release of hydrated silver ions during the process [37,38]. The properties of silver NPs are shown in table S2 (SI).

Table 2. The thickness and contact angle for Iron and silver NPs containing membranes

	Thickness (μm)	Contact Angle (°)
$PMAA_{47}$–$PMMA_{185}$, 15% w/w, Spheres containing 1.5 mL of 6.7 mg/mL Iron NPs	1.2	45
$PMAA_{47}$–$PMMA_{200}$, 17.5% w/w, Spheres containing 1.7 mL of 5.1 mg/mL Silver NPs	1.1	39
$PMAA_{47}$–$PMMA_{267}$, 15% w/w, Worms containing 0.7 mL of 6.7 mg/mL Iron NPs	1.3	44
$PMAA_{47}$–$PMMA_{273}$, 17.5% w/w, Worms containing 0.5 mL of 5.1 mg/mL Silver NPs	1.0	41
$PMAA_{47}$–$PMMA_{356}$, 15% w/w, Vesicles containing 0.9 mL of 6.7 mg/mL Iron NPs	2	45
$PMAA_{47}$–$PMMA_{400}$, 17.5% w/w, Vesicles containing 1.3 mL of 5.1 mg/mL Silver NPs	1.3	40

For antibacterial and filtration studies, two dosages of silver ions were used one with lower concentration (1 mL of polymeric NPs: 1.3 mL of silver NPs) and one with a higher level (1mL of polymeric NPs: 1.7 mL of silver NPs). The membranes with 2 dosages (lower and higher concentration of silver were filtered using water at pH 7.1 at 4 bar of upstream pressure (dead end mode) for 80 h. Permeate collected during filtration was analyzed using Atomic Absorption Spectroscopy (AAS), and the concentration of silver leached out is depicted in Fig.3. After 6 h of permeation, about 61 and 98 μg/L of silver ions were detected in permeate from membranes with lower and higher concentrations of silver. This number further reduced to 38 and 45 μg/L when the filtration time increased to 8 h (see inset of Fig. 3), which is within the range of toxicity

threshold [39]. For all antibacterial tests and filtration studies, the membranes were compacted for 8 h prior to use making sure that the antibacterial effect observed is due to the attached silver NPs in the matrix of polymeric NPs forming the membrane. The permeate was also analyzed by DLS (Dynamic light scattering), which confirmed no traces of silver or polymeric NPs.

To estimate the amount of silver NPs present on the membrane after leaching, a mass balance was carried out for membrane with lower and higher silver concentration. The concentration of leached silver in µg/h was plotted against time (h), and the area under the curve was estimated using trapezoidal rule (integration method)[40]. The area under the curve estimates the amount of silver NPs in µg lost from the membranes. The estimation confirmed the loss of about 4.42% of silver NPs for the 1st 8 h of operation under 4 bar of transmembrane pressure followed by further 4.07% loss of silver NPs, for the membrane with a lower concentration of silver confirming the presence of 91.51% of silver NPs remaining in membrane (Fig. 3A). For the membrane with higher concentration of silver (Fig. 3B), this loss was 5.7% in the 1st 8 h followed by a further 3.72% loss of silver NPs assuring the presence of 90.58% of silver NPs in the membrane.

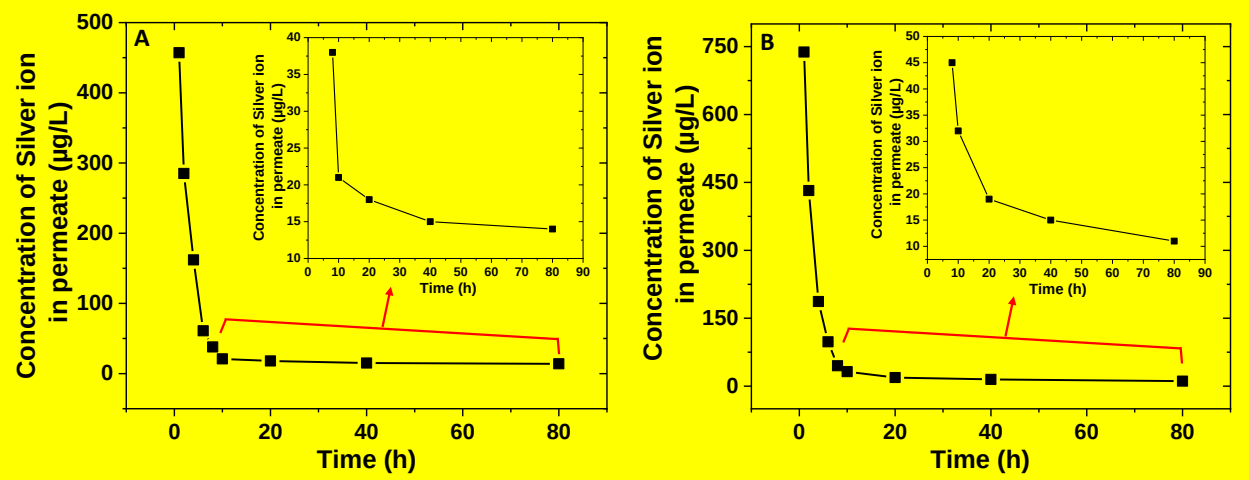

Fig. 3. Leaching out of silver ions from nanocomposite membranes containing (A) lower concentration of silver (1.3 mL of 5.1 mg/mL Silver NPs) (B) higher concentration of silver (1.7 mL of 5.1 mg/mL Silver NPs)

3.3.Antibacterial properties of the membrane

Antibacterial properties of pristine membranes from spheres, worms, and vesicles without any silver NPs revealed no biocidal activity. To test the biocidal activity of the nanocomposite membranes, only membranes made from spheres containing different dosages of silver NPs were selected using a gram-positive bacteria *Enterococcus hirae* as a model system. The inactivation kinetics of the bacteria with lower and higher concentrations of the silver NPs incorporated within the membranes was evaluated for various contact times (Fig. 4).

The concentration of the bacteria reduced from $1.15*10^6$ CFU/mL to $5.93*10^5$ CFU/mL at the end of 8^{th} h, which was further decreased to $1.26*10^4$ CFU/mL during 24 h of contact time for membrane with a lower concentration of silver NPs (Fig.4A). This decrease in number corresponds to 98.9%, which corresponds to almost 2 log decrease (Fig.4C) in the bacterial concentration after 24 h of contact time. When the silver concentration was increased to a higher level, the bacterial count decreased from $1.02*10^6$ CFU/mL to $2.0*10^3$ CFU/mL after 24 h of contact between the membranes and the solution with bacteria (Fig. 4B). This decrease in number corresponds to a 99.8% reduction, which is about 3 log decrease in the bacteria count after 24 h of contact (Fig.4C). When the concentration was additionally increased by 0.3 mL (yielding 2 ml of silver NPs), a 3 log decrease was achieved within 19 h of contact time. However, just 1.7 mL of silver NPs is enough to provide the required mechanical stability to the active layer. The duration of contact could be further decreased to 15 h when the concentration was also increased to 2.15 mL showing the importance of silver concentration in the membrane and the contact time.

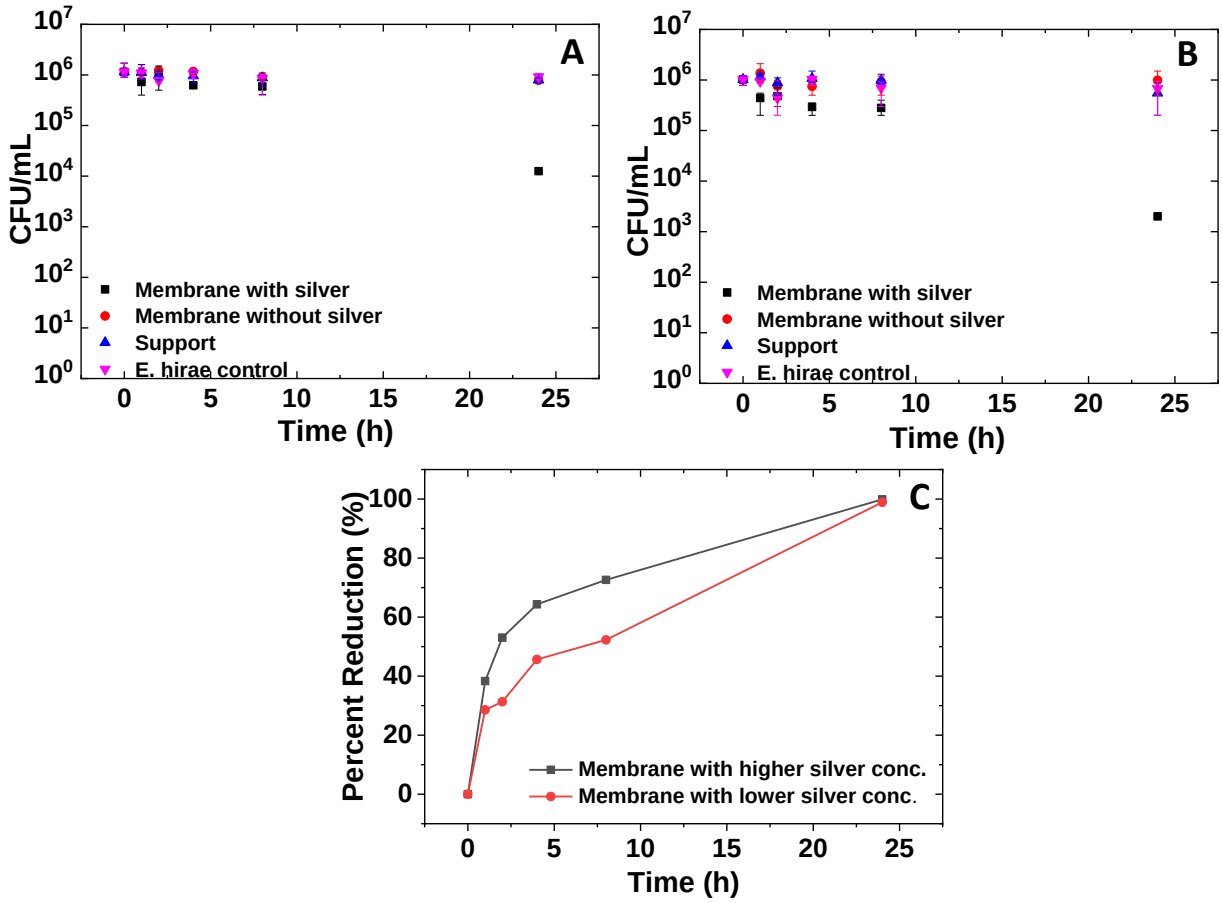

Fig. 4. Inactivation kinetics of *Enterococcus hirae* due to the incorporation of silver NPs in membranes made from casting solutions with different compositions: (A) Lower concentration of silver NPs (B) Higher concentration of silver NPs (C) Percent reduction of *Enterococcus hirae* for the two types of membrane tested.

3.4.Bacterial filtration studies

The cross-flow mode was selected over dead-end filtration since the cross-flow mode is less prone to fouling due to the direction of the fluid flow tangential to the membrane surface. The bacterial filtration studies using the membrane made from spherical NPs containing a lower and higher amount of silver NPs are shown in Fig. 5.

In this filtration assay, nylon membranes were used as a control, and all the experiments were carried out at 1.5 bar of TMP. The rejection factor of the reference nylon membranes for bacteria

was about 38-40%. The membrane containing a lower amount of silver NPs showed a rejection of 81%, and the membrane with a higher amount of silver NPs had a rejection of 96.3%. The rejection percentage is a clear indication that the bacteria has passed through the membrane due to the formation of larger pores since not enough silver NPs were present to keep the polymeric NPs together under the applied pressure (refer to the results obtained for water filtration). When the silver NPs added to the casting solution increased to 2.15 mL, the rejection of bacteria increased to 99.6%, indicating the control over the pore size.

The collected permeate showed a 1 log decrease (93% reduction) in the bacterial count for the membrane containing the lower amount of silver NPs and approximately 2 log decrease (98.4% reduction) for the membrane containing a higher amount of silver NPs. The retentate, as well as the feed stream, showed a slight decrease in the bacteria concentration for the membrane with a higher amount of silver NPs. We believe that this modest decrease in the bacterial count is due to insufficient contact time as well as the amount of silver NPs. During the experiment, about 50 mL of solution was filtered during 25 min with membranes with silver, not providing enough time for deactivation. The performance can be enhanced by increasing the silver concentration as well as keeping the bacterial solution in contact with the membrane for specific residence time. Since the membrane rejection is about 96.3% for higher silver NPs concentration, most of the bacteria will be retained in the retentate, leading to higher contact time with the membrane and, consequently, to a higher inactivation.

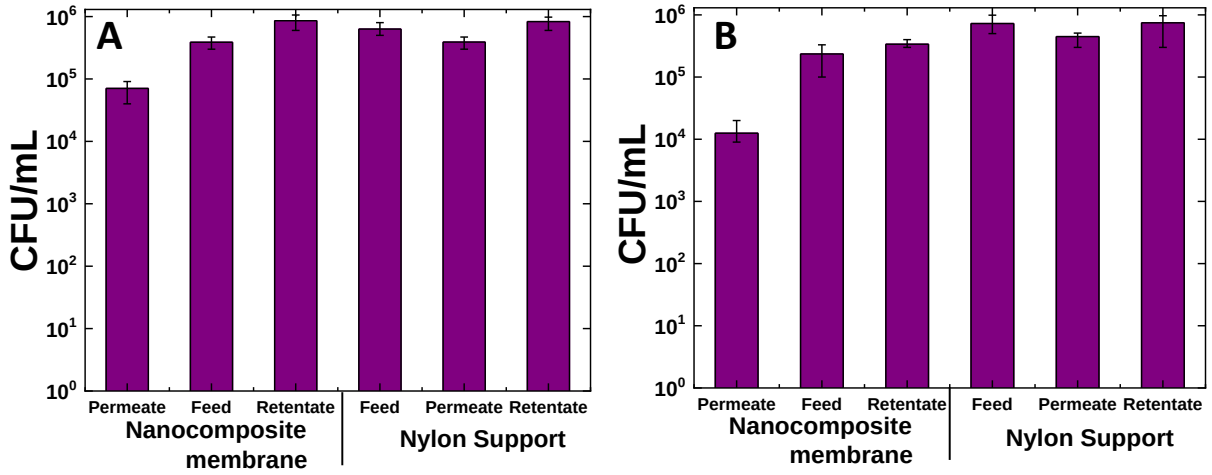

Fig. 5. Bacterial filtration studies with membranes made from spheres containing silver NPs with (A) Lower silver NPs(B) Higher silver NPs

To estimate the amount of silver NPs lost from membrane after compaction followed by bacterial filtration studies, mass balance of silver NPs carried out and shown in SI. For the bacterial filtration studies, the transmembrane pressure was reduced to 1.5 bar and filtration carried out. If the filtration is carried out continuously for 72 h (0-8 h for compaction at 4 bar followed by bacterial filtration 8-80 h), the loss of silver NPs estimated to be 5.41% and 6.49% for the membrane with the lower and the higher silver NPs respectively suggesting the presence of significant amount of silver NPs in membranes. As aimed, the technique proposed for the preparation of membranes with an effective bactericide effect was successful. A promising proof-of-concept was achieved. It should be emphasized that during the operating periods used in this work, no biofouling was observed. However, long-term studies (at least 1 to 2 years of operation) are required before claiming an effective solution.

4. CONCLUSION

In this work, we have used silver NPs as a bridging entity between the polymeric NPs made from $PMAA_{47}$-*b*-$PMMA_y$(where y = 195-spheres, 273-worms, and 368-vesicles) block copolymer synthesized using RAFT polymerization. These NPs have been used to make nanocomposite membranes. The nanocomposite membranes prepared showed excellent mechanical stability containing different amounts of inorganic NPs linking the polymeric NPs for all three different morphologies studied. At 4 bar of transmembrane pressure, the membranes from spheres exhibited the highest flux value (589.6 $L.h^{-1}.m^{-2}$), whereas the membranes from vesicles and worms showed a maximum flux of 411.9 $L.h^{-1}.m^{-2}$ and 277.5 $L.h^{-1}.m^{-2}$, respectively.

The contact time between the nanocomposite membranes and *E. hirae* to achieve 2-3 log inactivation depends on the concentration of silver NPs incorporated in the membranes. Membrane filtration of solutions spiked with bacteria also revealed that the silver incorporation within the membranes made from spherical polymeric NPs is crucial to increase the bacteria rejection due to their smaller pore size. Due to the high membrane retention rate, microorganisms will have high contact time with the membrane surface, which will lead to high inactivation. This work also needs further investigation on process effectiveness in real matrices, with natural organic matter and turbidity interference.

SUPPORTING INFORMATIONS

The supporting information contains Polymeric NPs characterization, flux and permeability data, mass balance of silver NPs in membrane and SEM images of membranes containing different proportions of polymeric and inorganic NPs.

Notes

The authors declare no competing financial interest.

ACKNOWLEDGEMENTS

The doctorate of L.U. has been completed at the Institut Europeen des Membranes and carried out in three universities:́ Université de Montpellier (France), Universidad de Zaragoza (Spain), and Universidade Nova de Lisboa (Portugal), and financed by a scholarship of the European Commission Education, Audiovisual and Culture Executive Agency (EACEA), under the program Erasmus Mundus Doctorate in Membrane Engineering, EUDIME (FPA No. 2011-0014, Edition III). D.Q. and M.S. acknowledge financial support from the "Agence Nationale pour la Recherche" (ANR-13- JS08-0008-01).

Financial support from Fundação para a Ciência e a Tecnologia through the PhD fellowship SFRH/BD/111150/2015 is gratefully acknowledged. iNOVA4Health-UID/Multi/04462/2013, a program financially supported by Fundação para a Ciência e Tecnologia/Ministério da Educação e Ciência, through national funds and co-funded by FEDER under the PT2020 Partnership Agreement, is also gratefully acknowledged. This work was also supported by the Associate Laboratory for Green Chemistry LAQV which is financed by national funds from FCT/MCTES (**UIDB/50006/2020**).

REFERENCES

[1] L. Upadhyaya, M. Semsarilar, S. Nehache, A. Deratani, D. Quemener, Filtration membranes from self-assembled block copolymers – a review on recent progress, Eur. Phys. J. Spec. Top. 224 (2015) 1883–1897. https://doi.org/10.1140/epjst/e2015-02507-7.

[2] L. Upadhyaya, C. Egbosimba, X. Qian, R. Wickramasinghe, R. Fernández-Pacheco, I.M. Coelhoso, C.A.M. Portugal, J.G. Crespo, D. Quemener, M. Semsarilar, Influence of Magnetic Nanoparticles on PISA Preparation of Poly(Methacrylic Acid)- *b* - Poly(Methylmethacrylate) Nano-Objects, Macromol. Rapid Commun. (2018) 1800333.

https://doi.org/10.1002/marc.201800333.

[3] A. Rubio, G. Desnos, M. Semsarilar, Nanostructured Membranes from Soft and Hard Nanoparticles Prepared via RAFT-mediated PISA, Macromol. Chem. Phys. 219 (2018) 1800351. https://doi.org/10.1002/macp.201800351.

[4] L. Upadhyaya, M. Semsarilar, R. Fernández-Pacheco, G. Martinez, R. Mallada, I.M. Coelhoso, C.A.M. Portugal, J.G. Crespo, A. Deratani, D. Quemener, Nano-structured magneto-responsive membranes from block copolymers and iron oxide nanoparticles, Polym. Chem. 8 (2017) 605–614. https://doi.org/10.1039/c6py01870j.

[5] L. Upadhyaya, M. Semsarilar, R. Fernández-Pacheco, G. Martinez, R. Mallada, A. Deratani, D. Quemener, Porous membranes from acid decorated block copolymer nano-objects via RAFT alcoholic dispersion polymerization, Polym. Chem. 7 (2016). https://doi.org/10.1039/c5py01888a.

[6] L. Upadhyaya, M. Semsarilar, S. Nehache, D. Cot, R. Fernández-Pacheco, G. Martinez, R. Mallada, A. Deratani, D. Quemener, Nanostructured Mixed Matrix Membranes from Supramolecular Assembly of Block Copolymer Nanoparticles and Iron Oxide Nanoparticles, Macromolecules. 49 (2016) 7908–7916. https://doi.org/10.1021/acs.macromol.6b01738.

[7] L. Upadhyaya, M. Semsarilar, D. Quémener, R. Fernández-Pacheco, G. Martinez, R. Mallada, I.M. Coelhoso, C.A.M. Portugal, J.G. Crespo, Block copolymer based novel magnetic mixed matrix membranes-magnetic modulation of water permeation by irreversible structural changes, J. Memb. Sci. 551 (2018) 273–282. https://doi.org/10.1016/j.memsci.2018.01.032.

[8] S. Nehache, M. Semsarilar, A. Deratani, M. In, P. Dieudonné-George, J. Lai Kee Him, P.

Bron, D. Quémener, Nano-porous structures *via* self-assembly of amphiphilic triblock copolymers: influence of solvent and molecular weight, Polym. Chem. 9 (2018) 193–202. https://doi.org/10.1039/C7PY01853C.

[9] S. Nehache, M. Semsarilar, A. Deratani, D. Quemener, S. Nehache, M. Semsarilar, A. Deratani, D. Quemener, Negatively Charged Porous Thin Film from ABA Triblock Copolymer Assembly, Polymers (Basel). 10 (2018) 733. https://doi.org/10.3390/polym10070733.

[10] S. Nehache, M. Semsarilar, M. In, P. Dieudonné-George, J. Lai-Kee-Him, P. Bron, D. Bouyer, A. Deratani, D. Quemener, Self-assembly of PS-PNaSS-PS triblock copolymers from solution to the solid state, Polym. Chem. 8 (2017) 3357–3363. https://doi.org/10.1039/C7PY00531H.

[11] S. Nehache, P. Tyagi, M. Semsarilar, A. Deratani, T.N.T. Phan, D. Gigmes, D. Quemener, Translocation across a self-healing block copolymer membrane, Soft Matter. 13 (2017) 6689–6693. https://doi.org/10.1039/C7SM01284E.

[12] S.P. Nunes, A. Car, From Charge-Mosaic to Micelle Self-Assembly: Block Copolymer Membranes in the Last 40 Years, Ind. Eng. Chem. Res. 52 (2013) 993–1003.

[13] S.P. Nunes, R. Sougrat, B. Hooghan, D.H. Anjum, A.R. Behzad, L. Zhao, N. Pradeep, I. Pinnau, U. Vainio, K. Peinemann, Ultraporous Films with Uniform Nanochannels by Block Copolymer Micelles Assembly, Macromolecules. (2010) 8079–8085. https://doi.org/10.1021/ma101531k.

[14] S.P. Nunes, M. Karunakaran, N. Pradeep, A.R. Behzad, B. Hooghan, R. Sougrat, H. He, K.-V. Peinemann, From Micelle Supramolecular Assemblies in Selective Solvents to Isoporous Membranes, Langmuir. 27 (2011) 10184–10190.

https://doi.org/10.1021/la201439p.

[15] S.P. Nunes, A.R. Behzad, B. Hooghan, R. Sougrat, M. Karunakaran, N. Pradeep, U. Vainio, K.-V. Peinemann, Switchable pH-Responsive Polymeric Membranes Prepared *via* Block Copolymer Micelle Assembly, ACS Nano. 5 (2011) 3516–3522. https://doi.org/10.1021/nn200484v.

[16] U. Farooq, L. Upadhyaya, A. Shakeel, G. Martinez, M. Semsarilar, pH-responsive nano-structured membranes prepared from oppositely charged block copolymer nanoparticles and iron oxide nanoparticles, J. Memb. Sci. (2020) 118181. https://doi.org/10.1016/j.memsci.2020.118181.

[17] M. Semsarilar, S. Perrier, "Green" reversible addition-fragmentation chain-transfer (RAFT) polymerization, Nat. Chem. 2 (2010) 811–820. https://doi.org/10.1038/nchem.853.

[18] L. Upadhyaya, M. Semsarilar, A. Deratani, D. Quemener, Nanocomposite Membranes with Magnesium , Titanium , Iron and Silver Nanoparticles - A Review, J. Membr. Sci. Res. 3 (2017) 187–198. https://doi.org/10.22079/jmsr.2017.23779.

[19] L. Upadhyaya, X. Qian, S. Ranil Wickramasinghe, Chemical modification of membrane surface — overview, Curr. Opin. Chem. Eng. 20 (2018) 13–18. https://doi.org/10.1016/j.coche.2018.01.002.

[20] N.L. Le, S.P. Nunes, Materials and membrane technologies for water and energy sustainability, Sustain. Mater. Technol. 7 (2016) 1–28. https://doi.org/10.1016/j.susmat.2016.02.001.

[21] J.-M. Laîné, D. Vial, P. Moulart, Status after 10 years of operation — overview of UF technology today, Desalination. 131 (2000) 17–25. https://doi.org/10.1016/S0011-

9164(00)90002-X.

[22] F. Meng, S. Zhang, Y. Oh, Z. Zhou, H.-S. Shin, S.-R. Chae, Fouling in membrane bioreactors: An updated review, Water Res. 114 (2017) 151–180. https://doi.org/10.1016/J.WATRES.2017.02.006.

[23] L.-Q. Shen, Z.-K. Xu, Z.-M. Liu, Y.-Y. Xu, Ultrafiltration hollow fiber membranes of sulfonated polyetherimide/polyetherimide blends: preparation, morphologies and anti-fouling properties, J. Memb. Sci. 218 (2003) 279–293. https://doi.org/10.1016/S0376-7388(03)00186-8.

[24] H. Basri, A.F. Ismail, M. Aziz, K. Nagai, T. Matsuura, M.S. Abdullah, B.C. Ng, Silver-filled polyethersulfone membranes for antibacterial applications — Effect of PVP and TAP addition on silver dispersion, Desalination. 261 (2010) 264–271. https://doi.org/10.1016/j.desal.2010.05.009.

[25] X. Cao, M. Tang, F. Liu, Y. Nie, C. Zhao, Immobilization of silver nanoparticles onto sulfonated polyethersulfone membranes as antibacterial materials, Colloids Surfaces B Biointerfaces. 81 (2010) 555–562. https://doi.org/10.1016/j.colsurfb.2010.07.057.

[26] F. Diagne, R. Malaisamy, V. Boddie, R.D. Holbrook, B. Eribo, K.L. Jones, Polyelectrolyte and Silver Nanoparticle Modification of Microfiltration Membranes To Mitigate Organic and Bacterial Fouling, Environ. Sci. Technol. 46 (2012) 4025–4033. https://doi.org/10.1021/es203945v.

[27] Y. Kim, D. Rana, T. Matsuura, W.J. Chung, Towards antibiofouling ultrafiltration membranes by blending silver containing surface modifying macromolecules, Chem. Commun. 48 (2012) 693–695. https://doi.org/10.1039/c1cc16217a.

[28] A. Gupta, K. Matsui, J.-F. Lo, S. Silver, Molecular basis for resistance to silver cations in

Salmonella, Nat. Med. 5 (1999) 183–188. https://doi.org/10.1038/5545.

[29] T.C. Prathna, N. Chandrasekaran, A.M. Raichur, A. Mukherjee, Biomimetic synthesis of silver nanoparticles by Citrus limon (lemon) aqueous extract and theoretical prediction of particle size, Colloids Surfaces B Biointerfaces. 82 (2011) 152–159. https://doi.org/10.1016/j.colsurfb.2010.08.036.

[30] J.S. Kim, E. Kuk, K.N. Yu, J.-H. Kim, S.J. Park, H.J. Lee, S.H. Kim, Y.K. Park, Y.H. Park, C.-Y. Hwang, Y.-K. Kim, Y.-S. Lee, D.H. Jeong, M.-H. Cho, Antimicrobial effects of silver nanoparticles, Nanomedicine Nanotechnology, Biol. Med. 3 (2007) 95–101. https://doi.org/10.1016/j.nano.2006.12.001.

[31] Q. Li, S. Mahendra, D.Y. Lyon, L. Brunet, M. V. Liga, D. Li, P.J.J. Alvarez, Antimicrobial nanomaterials for water disinfection and microbial control: Potential applications and implications, Water Res. 42 (2008) 4591–4602. https://doi.org/10.1016/j.watres.2008.08.015.

[32] P. Madhavan, P.-Y. Hong, R. Sougrat, S.P. Nunes, Silver-Enhanced Block Copolymer Membranes with Biocidal Activity, ACS Appl. Mater. Interfaces. 6 (2014) 18497–18501. https://doi.org/10.1021/am505594c.

[33] A. Dasari, J. Quirós, B. Herrero, K. Boltes, E. García-Calvo, R. Rosal, Antifouling membranes prepared by electrospinning polylactic acid containing biocidal nanoparticles, J. Memb. Sci. 405–406 (2012) 134–140. https://doi.org/10.1016/j.memsci.2012.02.060.

[34] X. Deng, A.Y. Nikiforov, T. Coenye, P. Cools, G. Aziz, R. Morent, N. De Geyter, C. Leys, Antimicrobial nano-silver non-woven polyethylene terephthalate fabric via an atmospheric pressure plasma deposition process., Sci. Rep. 5 (2015) 10138. https://doi.org/10.1038/srep10138.

[35] S. Jeon, S. Rajabzadeh, R. Okamura, T. Ishigami, S. Hasegawa, N. Kato, H. Matsuyama, The Effect of Membrane Material and Surface Pore Size on the Fouling Properties of Submerged Membranes, Water. 8 (2016) 602. https://doi.org/10.3390/w8120602.

[36] S.Y. Park, Y.J. Kim, S.-Y. Kwak, L. Chen, J. You, H. Frey, P.J.J. Alvarez, Versatile surface charge-mediated anti-fouling UF/MF membrane comprising charged hyperbranched polyglycerols (HPGs) and PVDF membranes, RSC Adv. 6 (2016) 88959–88966. https://doi.org/10.1039/C6RA19020K.

[37] J.-H. Li, X.-S. Shao, Q. Zhou, M.-Z. Li, Q.-Q. Zhang, The double effects of silver nanoparticles on the PVDF membrane: Surface hydrophilicity and antifouling performance, Appl. Surf. Sci. 265 (2013) 663–670. https://doi.org/10.1016/J.APSUSC.2012.11.072.

[38] J. Liu, R.H. Hurt, Ion Release Kinetics and Particle Persistence in Aqueous Nano-Silver Colloids, Environ. Sci. Technol. 44 (2010) 2169–2175. https://doi.org/10.1021/es9035557.

[39] H. Cao, Silver nanoparticles for antibacterial devices : biocomparibility and toxicity, CRC Press, 2017.

[40] M. Schrag, K. Regal, Pharmacokinetics and Toxicokinetics, in: A Compr. Guid. to Toxicol. Preclin. Drug Dev., Elsevier Inc., 2013: pp. 31–68. https://doi.org/10.1016/B978-0-12-387815-1.00003-4.